GI_Forum 2017, Issue 1
Page: 79 - 92
Full Paper
Corresponding Author:
bruns@fzi.de
DOI: 10.1553/giscience2017_01_s79

# Stable Hotspot Analysis for Intra-Urban Heat Islands

Julian Bruns and Viliam Simko

FZI Forschungszentrum Informatik am Karlsruher Institut für Technologie,
Karlsruhe, Germany

**Abstract**

The Urban Heat Island (UHI) effect describes the difference in temperature between cities and their surrounding areas. However, temperature differences within city limits, so-called Intra-Urban Heat Islands (IUHI), affect human health as well as the energy demands in local areas. In order to anticipate and mitigate the resulting impacts of heat through urban planning, a method to reliably detect these local areas is needed. Existing methods from the geo-statistical field can identify these areas. But these statistics, depending on their parametrization, can be unstable in their detection of hotspots, in particular temperature hotspots. In this paper, we propose a modification of the well-known Getis-Ord ($G^*$) statistic, called the Focal $G^*$ statistic. This modification replaces the computation of the global mean and standard deviation with their focal counterparts. We define the stability of our approach by introducing a stability metric called Stability of Hotspot (SoH), which requires that hotspots have to be in similar areas regardless of the chosen weight matrix. The results are evaluated on real-world temperature data for the city of Karlsruhe.

**Keywords:**

Urban Heat Island, Intra-Urban Heat Island, Hotspot Analysis, Stability Metric

## 1 Introduction

For urban city planners, the detection of Intra-Urban Heat Islands (IUHI) is of great interest as high temperatures impact energy consumption (Hassid et al., 2000) as well as human health (Ye et al., 2012). The effect that the temperatures between an urban area and its surroundings differ, called the Urban Heat Island effect (Oke, 1982), has long been the subject of research. Historically, however, most studies had to rely on a few, fixed weather stations, low spatio-temporal resolution of satellite imagery, or small-scale mobile measurements by car, preventing the modelling of finer-grained temperature differences within an urban area itself. With the advent of, among other technological advances, inexpensive mobile sensors, higher spatio-temporal resolution of satellite imagery, and volunteered geographic information, it is now feasible to focus on the temperature differences in a city as the subject of interest.

Hotspot analysis is a tool which is suited for the detection of such areas. In the context of IUHI, we can detect those precise areas where the temperature is significantly different from the mean temperature of the study area as a whole. This enables us to identify points of interest without the need to pre-process the data.

Although existing methods are independent of concrete values, their results are highly dependent on the size of the study area and on their parametrization, such as the weight matrix in the case of the Getis-Ord statistic. This dependency can lead to unstable hotspots, where the hotspots identified appear only in one specific combination of parameters. The generalization of insights gained from unstable hotspots is suboptimal. A city planner who has to rely on those insights will most likely prioritize the wrong area to invest limited city resources. Given the increasing importance of detecting extreme local temperatures in cities (see e.g. Hansen et al., 2010; Chase et al., 2006; United Nations, 2014), means are needed to reliably detect and mitigate the effects of temperature extremes in a proactive fashion.

To solve this problem, we first propose a metric, which we call Stability of Hotspot (SoH), to measure the stability of a hotspot analysis by considering the parametrization of the weight matrix. This metric measures whether a hotspot found for a given weight matrix is carried over to the found hotspots with different weight matrices. This enables us to quantify the stability of any hotspot analysis. Based on our understanding of the instability of existing hotspot analyses, we propose a modification of the well-known Getis-Ord statistic ($G^*$): the Focal Getis-Ord statistic (Focal $G^*$). Instead of the global mean and variance used by $G^*$, Focal $G^*$ uses only the mean and variance of a predefined region around each point. This region is a subset of the whole study area. By doing this, the instability is contained within a smaller region and is thereby independent of the parametrization of the weight matrix. We test our stability metric as well as this modified approach on data given by two temperature snapshots of the city of Karlsruhe taken in 2008.

## 2 Related work

### Urban Heat Island

Scientific interest in the phenomenon of UHI is well established. One of the earliest known overviews of the scientific literature on city climates is given by Albert Kratzer (1937). At that time, relations between temperature, humidity, human heat fluxes and air pollution were already being investigated.

A more recent overview comes from Arnfied (2003). The focus here lies on developments in the field of climatology between 1980 and 2003. In particular, the rise of simulations and modelling is lauded, but, to quote Arnfield, 'simple methods are still needed to estimate UHI intensity within urban areas' (p. 18).

Schwarz, Lautenbach and Seppelt (2011) compare 11 different Surface Urban Heat Island (SUHI) indicators, on a dataset of 263 European cities. They show that the selection of indicators is important for the detection of UHI due to possible instabilities of each indicator.

A more recent development is the focus on IUHI, the definition of which comes from Martin, Baudouin and Gachon (2015). By defining temperature thresholds with respect to spatial reference, the thresholds enable the detection of hotspots in a city, which Martin et al. call surface intra-UHI. Their method comes down to five basic steps, and is essentially a comparison of absolute deviation from the mean temperature of the survey area. The results can then be used to detect areas of interest in a city and potentially trigger alerts for a much finer spatial granularity.

While the proposition to examine urban micro-climates can be traced back as far as 1937 (Kratzer, 1937), we have found few studies in this field. Schwarz et al. (2012) state that the reduction of a UHI to a single value for a whole city is questionable where its explanatory power is concerned. But they also state that there is currently no other way to quantify the differences amongst different cities.

The difficulties presented by comparing the UHI values for different cities are addressed by Stewart and Oke (2012). They propose the use of local climate zones (LCZ) to standardize the methodology and terminology.

Subsurface temperatures are another feature of urban areas that affect temperature distribution. Menberg et al. (2013) look into the distribution of the temperatures below the surface – the subsurface temperatures – and find local hotspots, related to local heat sources, with deviations of up to +20° Kelvin.

## Hotspot Analysis

The goal of an analysis of temperatures in a city is to find the most interesting, significant areas, i.e. hotspots (Martin, Baudouin and Gachon, 2015). This goal is similar to hotspot analysis in the field of geo-statistics. One of the most fundamental approaches is Moran's I (Moran, 1950), which tests whether or not a spatial dependency exists and gives the information on global dependencies in a data set. Several geo-statistical tests are based on this hypothesis test. The best known are the Getis-Ord statistic (Ord and Getis, 1995) and LISA (Anselin, 1995). In both cases, the general, global statistic of Moran's I is applied in a local context. The goal is to detect not only global values, but also to focus on local hotspots and to measure the significance of these local areas.

The local Getis-Ord statistic (Ord and Getis 1995) is defined as follows:

**Definition 1 (Getis-Ord $G^*$statistic).** Assuming a study area with $n$ measurements, let $X = [x_1, \dots, x_n]$ be all values measured in this area. Let $w_{i,j}$ be a spatial weight between two points $i$ and $j$ for all $i, j \in \{1, \dots, n\}$. The Getis-Ord $G_i^*$ statistic is given as:

$$G_i^* = \frac{\sum_{j=1}^{n} w_{i,j}\, x_j - \overline{X} \sum_{j=1}^{n} w_{i,j}}{S \sqrt{\frac{n \sum_{j=1}^{n} w_{i,j}^2 - (\sum_{j=1}^{n} w_{i,j})^2}{n-1}}}$$

where:

- $\overline{X}$ is the mean of all measurements
- $S$ is the standard deviation of all measurements.

This statistic creates a z-score, which denotes the significance of an area in relation to its surrounding areas.

LISA is quite similar, as it is the local statistic for Moran's I (Anselin, 1995), but the z-score has a different meaning. In contrast to $G_i^*$, LISA does not distinguish between cold spots and hotspots, as it assigns high z-scores to most similar areas.

Two other well-known methods are the kernel density estimation (Pulugurtha, Krishnakumar and Nambisan, 2007) and kriging (Oliver and Webster, 1990). These do not provide significance levels. Instead, they estimate the values for each location based on the rest of the study area and a threshold value (Thakali, Kwon and Fu, 2015). Therefore, results for different areas are not comparable, especially in the case of differing temperature distributions. Kriging was developed for the estimation of ore deposits (Krige, 1951), but applications for geo-temporal forecasts with this approach can now be found, e.g. for the city of Zurich.[1]

All of the aforementioned methods use weights between pairs of points, usually based on their geographical distance. However, in real applications, the points are aggregated into rasters and the weights are represented as a weight matrix. This allows the algorithms to be expressed in terms of map algebra operations, a term first coined by Dana Tomlin (1990), and to be computed in a distributed fashion (e.g. using the Geotrellis framework running on Apache Spark (Eclipse Foundation, Azavea, and contributors, 2016)).

In the present study, we focus on the Getis-Ord statistic applied to raster representations of land surface temperature. This enables us to transform the formula for the $G^*$ statistic into a computationally more efficient form. We then propose a modification of the standard $G^*$ statistic, to increase the stability of the hotspots found.

## 3 Stability of Hotspot Analysis

Existing methods to determine hotspots are dependent on the parametrization of the weight matrix as well as on the size of the study area.

Consider the real-world example depicted in Figure 1. The temperature map of a morning thermal flight dataset (Figure 1a) has been processed using $G^*$ with an increasing size of weight matrix (Figures 1b, 1c and 1d).

1 https://r-video-tutorial.blogspot.de/2015/08/spatio-temporal-kriging-in-r.html

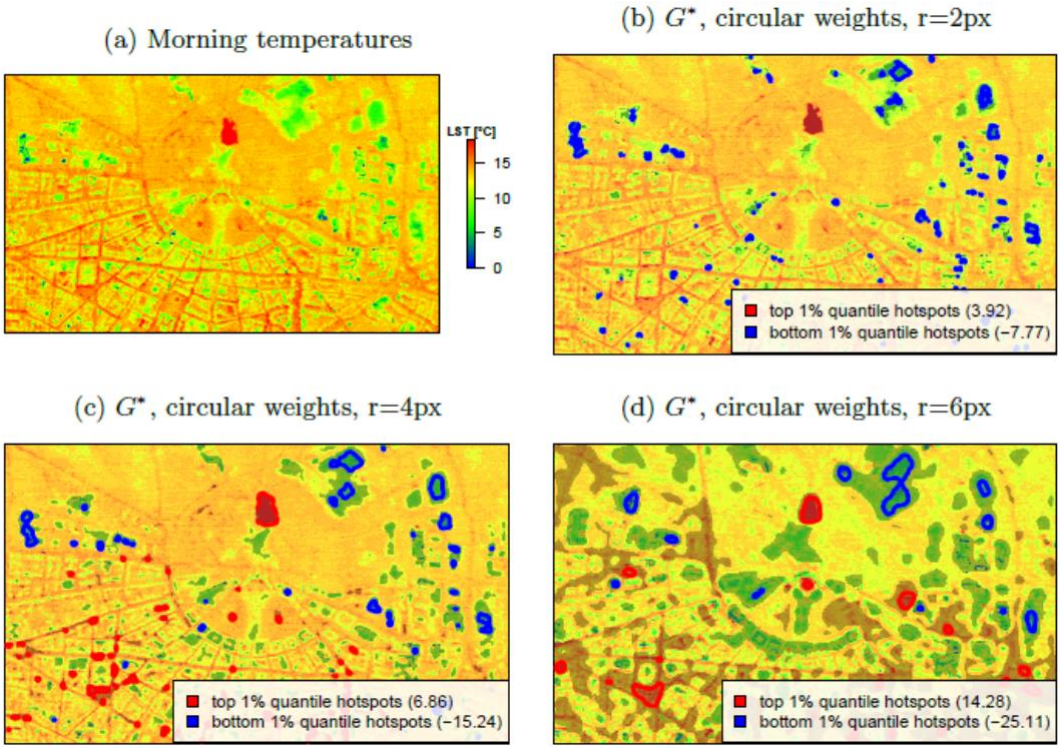


**Figure 1:** Karlsruhe city center. Selected area of 2.4 x 1.4 km. Pxel size 5x5 m

As we can see, hotspots often disappear, or appear to be unrelated to previously found hotspots. While these computations indeed show hotspots and the results are correct, they lack stability.

For a data analyst exploring the data interactively by choosing different filter sizes (in the form of matrices), it is important that the hotspot's position and size should change in a predictable manner. This intuition is the basis for our stability metric.

We define a hotspot that is found in comparably coarser resolutions as a parent (larger weight matrix), and in finer resolutions as a child (smaller weight matrix). To be stable, one assumes that every parent has at least one child and that each child has one parent. For a perfectly stable interaction, it can easily be seen that the connection between parent and child is an injective function, and between child and parent a surjective function. To measure the closeness of connection, we propose a metric called the Stability of Hotspot (SoH). It measures the deviation from a perfectly stable transformation of resolutions.

In its downward property (from parent to child; injective) it is defined as:

$$\text{Equation 1: } \text{SoH}^{\downarrow} = \frac{\text{ParentsWithChildNodes}}{\text{Parents}} = \frac{|\text{Parents} \cap \text{Children}|}{|\text{Parents}|}$$

and for its upward property (from child to parent; surjective):

$$\text{Equation 2: } \mathrm{SoH}^{\uparrow} = \frac{\mathrm{ChildrenWithParent}}{\mathrm{Children}} = 1 - \frac{|\mathrm{Children} - \mathrm{Parents}|}{|\mathrm{Children}|}$$

where $\mathrm{ParentsWithChildNodes}$ is the number of parents that have at least one child, $\mathrm{Parents}$ is the total number of parents, $\mathrm{ChildrenWithParent}$ is the number of children, and $\mathrm{Children}$ is the total number of children. The SoH is defined for a range between 0 and 1, where 1 represents a perfectly stable transformation while 0 would be a transformation with no stability at all.

## 4 Focal Getis-Ord

### Dataset

The two datasets (morning and evening flights) depicted in Figures 4 and 5 were obtained from thermal flights over the city of Karlsruhe on 26.09.2008 at 6:30–7:45 and 20:00–21:30. The flights were executed by the Nachbarschaftsverband Karlsruhe[2]. A single pixel in the raster represents an area of approximately $5 \times 5\mathrm{m}$. The whole dataset of size $35 \times 25\,\mathrm{km}$ was cropped into the inner-city area of $2.4 \times 1.4\mathrm{km}$. The temperatures in our dataset range from -1.7°C to +18.3°C. Missing values in the dataset were interpolated using a focal median function with a square matrix of 11x11 pixels, mainly for speeding up further computations and to avoid the special handling of NA values.

### Method

In what follows, we use the notation $\mathrm{R} \overset{\mathrm{op}}{\circ} \mathrm{M}$ to denote a focal operation $\mathrm{op}$ applied on a raster $\mathrm{R}$ with a focal window determined by a matrix $\mathrm{M}$. This is roughly equivalent to a command focal(x=R, w=M, fun=op) from the raster package in the R programming language (Hijmans 2016).

**Definition 2 ($\mathrm{G}^*$function on rasters).** The function $\mathrm{G}^*$ can be expressed as a raster operation:

$$G^*(R, W, st) = \frac{R \overset{\mathrm{sum}}{\circ} F - \mathrm{M} \sum_{w \in W} w}{S \sqrt{\frac{n \sum_{w \in W} w^2 - (\sum_{w \in W} w)^2}{N}}}$$

2 http://www.nachbarschaftsverband-karlsruhe.de/

where:

- R is the input raster
- W is a weight matrix of values between 0 and 1
- $st = (N, M, S)$ is a parametrization specific to a particular version of the $G^*$ function (Definitions 3 and 4).

**Definition 3 (Standard $G^*$ parametrization).** $G^*$ parametrization computes the parametrization st as global statistics for all pixels in the raster R:

- N represents the number of all pixels in R
- M represents the global mean of R
- S represents the global standard deviation of all pixels in R.

**Definition 4 (Focal $G^*$ parametrization).** Let F be a boolean matrix such that: $\text{all}(\dim(F) \geq \dim(W))$. This version uses focal operations to compute per-pixel statistics given by the focal neighbourhood F as follows:

- N is a raster computed as a focal operation $R \overset{\text{sum}}{\circ} F$. Each pixel represents the number of pixels from R convoluted with the matrix F.
- M is a raster computed as a focal mean $R \overset{\text{mean}}{\circ} F$. Thus each pixel represents the mean value of its F-neighbourhood.
- S is a raster computed as a focal standard deviation $R \overset{\text{sd}}{\circ} F$. Thus each pixel represents the standard deviation of its F-neighbourhood.

Figures 4 and 5 show Standard and Focal $G^*$ computations for both morning and evening datasets with weight matrix W of size 3, 5, 7, 9, 15 and 31. In these Figures, when computing Focal $G^*$, the focal matrix F has a constant size of $61 \times 61$ cells. An example weight matrix W and focal matrix F are depicted in Figure 3.

To evaluate the stability of our proposed Focal $G^*$, we compare it to two baselines:

- Standard $G^*$, which uses the same weight matrix W as our focal version
- Standard $G^*$, which uses a square weight matrix with all cells set to 1.
- d $G^*$, which uses a square weight matrix with all cells set to 1.

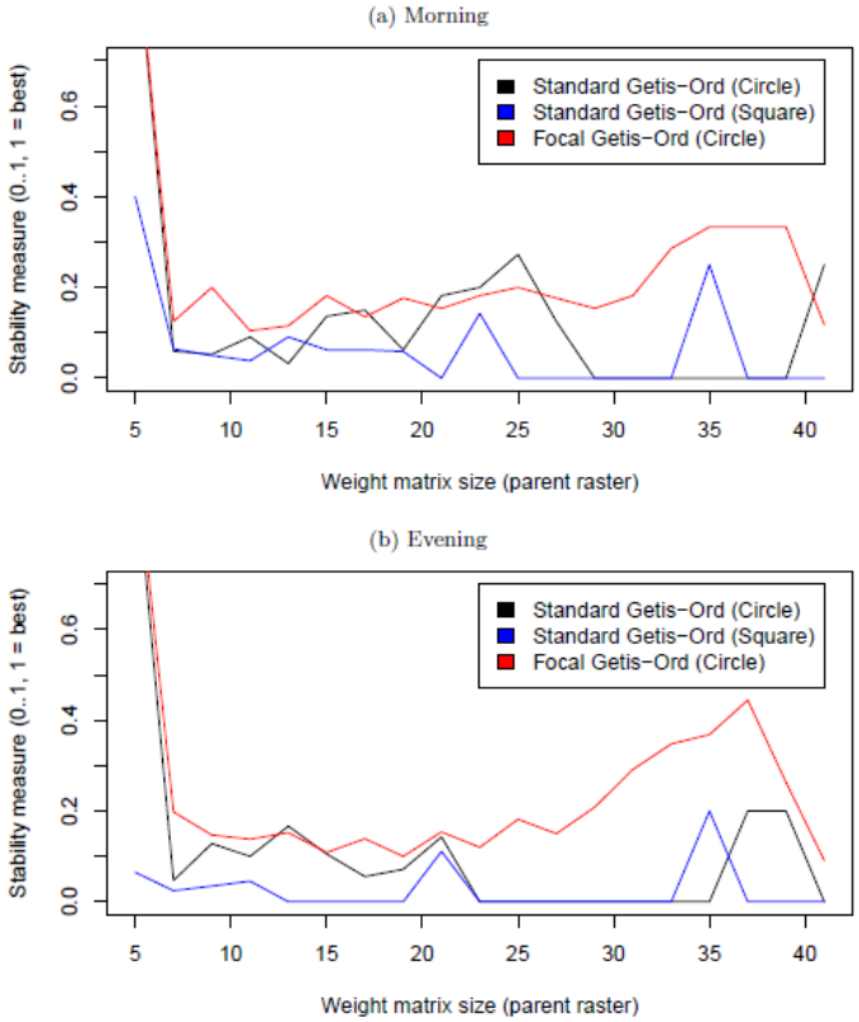


**Figure 2:** Evaluation results – Standard vs Focal G*

The evaluation results are plotted in Figure 2, where each point in the graph represents the $SoH^{\uparrow}$ metric (Equation 2) between two $G^*$ generated using weight matrices of sizes $i$ and $i + 2$. The focal matrix F has a fixed size of $41 \times 41$

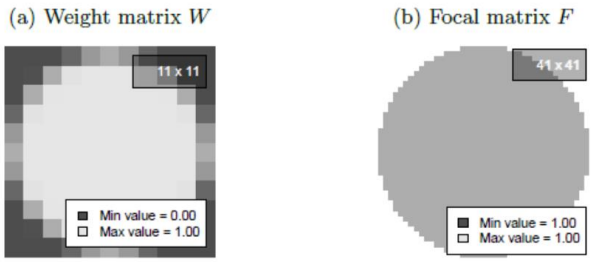


**Figure 3:** Example matrices *W* and *F*

## 5 Results and Discussion

The results for the hotspot analysis are found in Figures 4 and 5 for a comparison of the Standard $G^*$ and Focal $G^*$ statistics. It can easily be seen that both versions produce similar results, but the focal version produces a more differentiated picture for larger weight matrices. Small differences on a global scale are more pronounced on a regional scale and result in smaller and finer areas for hotspots. This enables the detection of additional hotspots and interesting areas which are most easily observable for the weight matrix of size $7 \times 7$ in the evening (Figure 5). This itself enables the detection of significant deviations from the surrounding area. In contrast, the Standard $G^*$ statistic shows larger areas as important. Therefore, depending on the needs of a planner, the Focal $G^*$ statistic is more helpful for identifying individual areas of interest, whereas the standard $G^*$ statistic gives a broader overview. For the identification of IUHI, this is quite important. If a city planner wishes to detect critical areas, it is important to detect not only general hot areas, but also those points where the most extreme differences in a local context exist. Finding these areas can help to identify the underlying causes, or to plan individual solutions.

These images also reveal that the hotspots found by the Focal $G^*$ statistic seem to be more stable. Because of limited space here, we compare their stability using only the $\mathrm{SoH}^{\uparrow}$. A plot of the results can be found in Figure 2, which compares the $\mathrm{SoH}^{\uparrow}$ between the increasing sizes of the weight matrix W. It is apparent that the typical implementation with a square weight matrix is the most unstable hotspot analysis, regardless of the time of day. This is to be expected as the binary weights increase the dependence on the weight matrix. The use of a decreasing weight matrix performs better. As the more outlying data points are given less weight, this reduces the dependence on the weight matrix and therefore leads to more stable results. Our proposed Focal $G^*$ statistic achieves the most stable results in almost all cases. Only data points in a restricted region around the area of interest may influence the significance level of the result. Through this restriction, high values at key points gain more weight regardless of the weight matrix and are therefore more independent of the weight matrix. This increases the stability. The decrease in stability for the largest weight matrices is most likely a result of the parametrization of the focal matrix. With the increasing size of the weight matrix in relation to the focal matrix, the value of each pixel comes closer to the mean of the area of the weight matrix. As can be seen easily from Definition 2, the value for every pixel would then be zero.

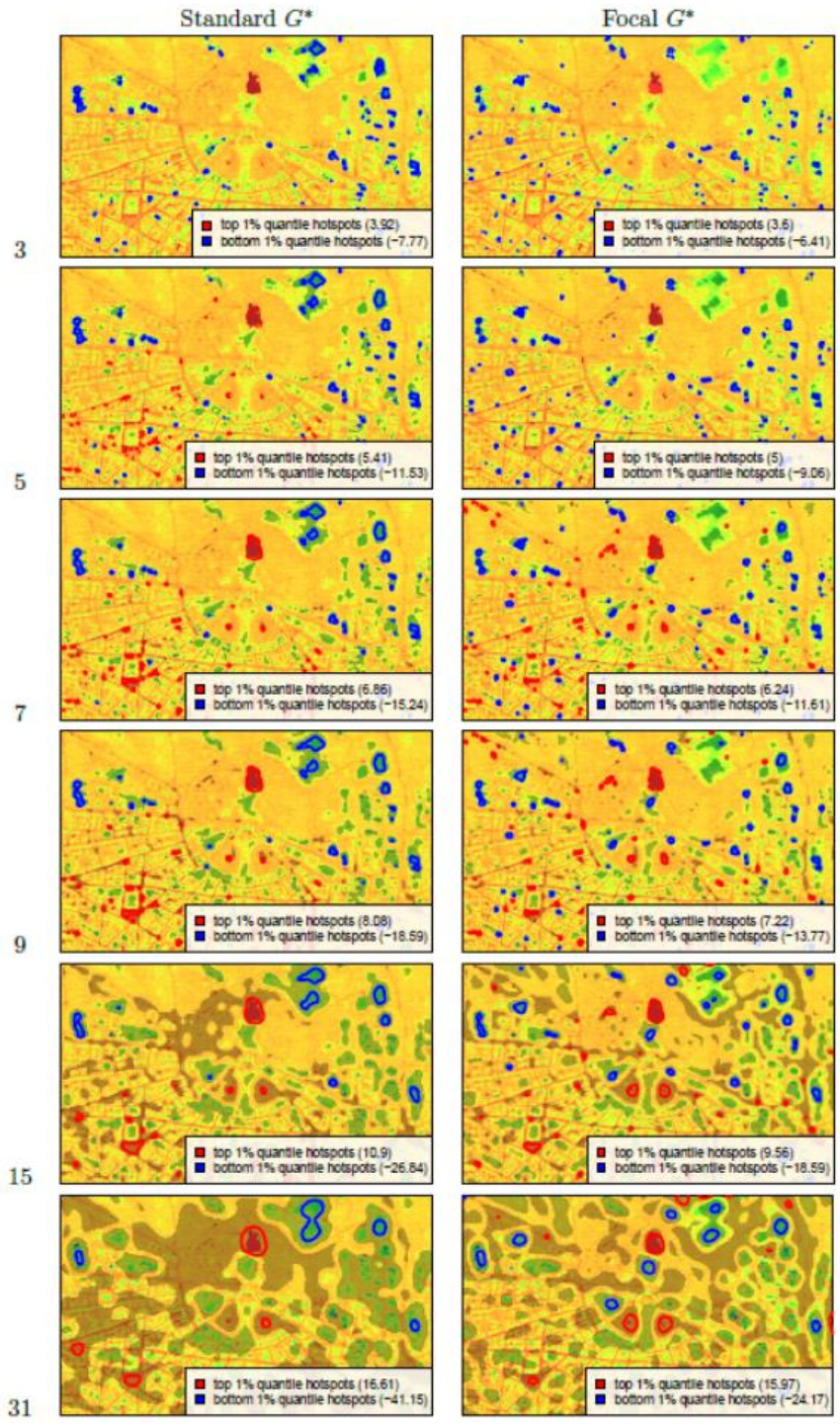


**Figure 4:** Standard and Focal G* with different weight matrices applied on morning dataset

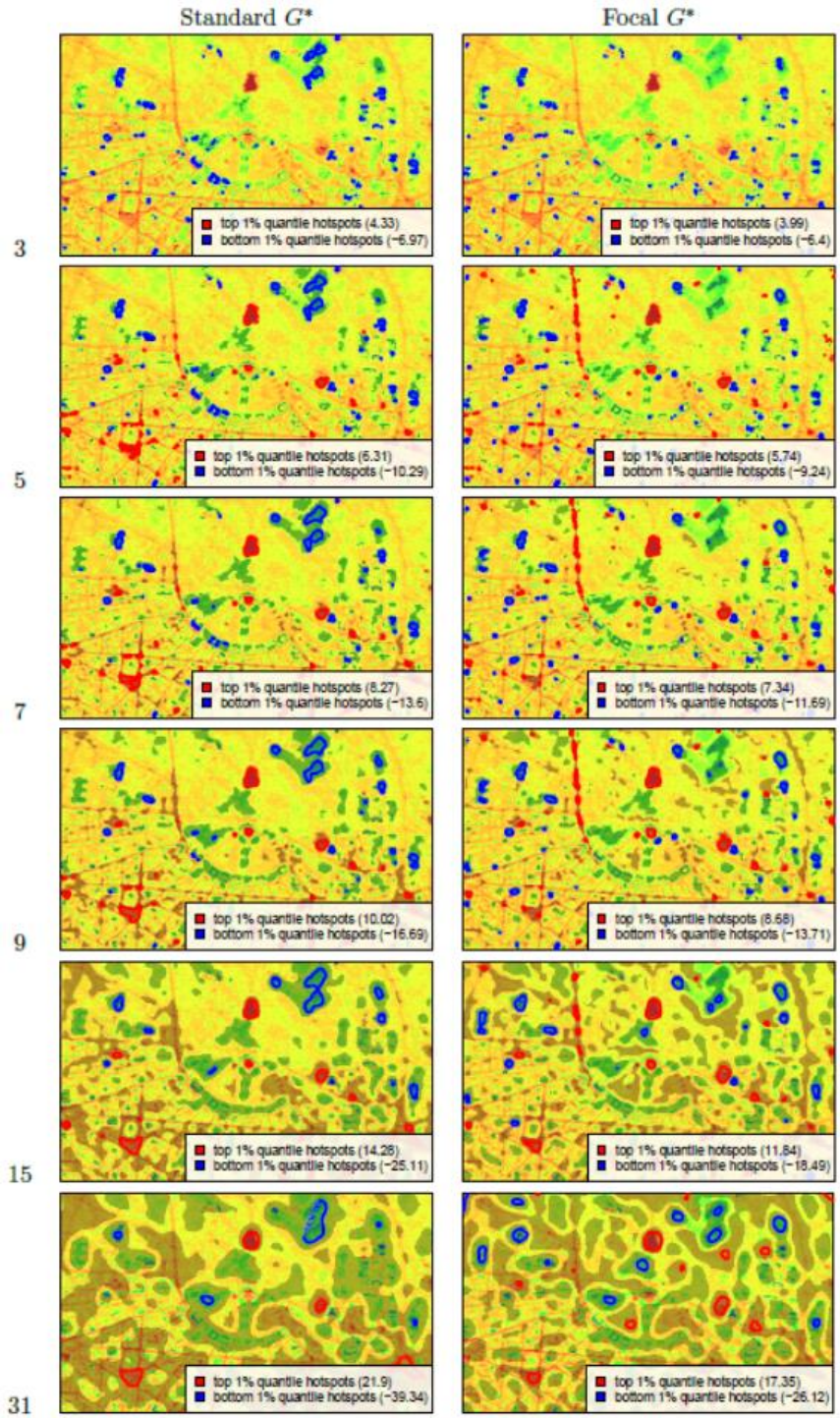


**Figure 5:** Standard and Focal G* with different weight matrices applied on evening dataset

## 6 Conclusions and Future Work

In this paper, we generalized the Getis-Ord statistic to deal with the problem of stability inherent in hotspot analysis. We identified possible underlying reasons for this instability: the weight matrix as well as the size of the study area. We developed a modified approach that deals with these two factors. The result is a modified $G^*$ statistic called the Focal $G^*$ statistic. It reduces the study area used for comparison into regions, and thereby achieves an increase in stability. To determine the effectiveness of our approach, we propose a stability metric for hotspots, called SoH. To our knowledge, no such metric existed before this work. The SoH computes the ratio of dependence of hotspots for different parametrizations of weight matrices. It enables the expression of the stability between each parametrization using a single value, between zero and one. Based on this number, one can decide which parametrization to use and researchers can compare the stability of their methods for unsupervised hotspot analyses. For temperature values in particular, one wishes to detect those areas which have high differences, regardless of a particular parametrization. If a hotspot appears for one parametrization only, the information gained for general use is quite small and can even lead to an inefficient allocation of resources.

This research has several restrictions which should be taken into account. First, we only tested the $SoH^{\uparrow}$ metric. While we assume, based on our graphical analysis, that the $SoH^{\downarrow}$ stability should be similar, we have no hard results. The results themselves are tested on two events in time for a fixed area of the city of Karlsruhe. We have not tested our approach on smaller or larger study areas, but we assume that the stability of the Focal $G^*$ would stay the same, whereas the stability of the $G^*$ statistic would increase with a smaller study area and decrease with a larger study area. This follows the reasoning that the impact of a single point increases with a decrease of the study area. To test this dependency is an interesting task for future work. The last restriction is the fixed size of the focal matrix for the Focal $G^*$ approach. We only tested one size in this study, but it is highly probable that the size of the focal matrix has an impact on the stability, as can be seen in Figure 2. While an overall trend can be seen when the size of the weight matrix W and the focal matrix F are almost identical, the exact ratio is beyond the scope of this work. Determining the optimal ratio of weight matrix W to focal matrix F as well as pinpointing when the stability suffers from those matrices being too similar in size are interesting questions for future work.

## Acknowledgements

This work is part of the research project BigGIS (reference number: 01IS14012) funded by the Federal Ministry of Education and Research (BMBF) within the frame of the programme 'Management and Analysis of Big Data' in 'ICT 2020 – Research for Innovations'. We thank the Nachbarschaftsverband Karlsruhe for the data from the thermal flights over Karlsruhe. R-packages used: raster (Hijmans, 2016), knitr (Xie, 2014).

## References

Anselin, L. (1995). Local Indicators of Spatial Association - Lisa. Geographical Analysis 27 (2): 93–115. doi:10.1111/j.1538-4632.1995.tb00338.x.

Arnfield, A. J. (2003). Two decades of urban climate research: a review of turbulence, exchanges of energy and water, and the urban heat island. International Journal of Climatology 23 (1): 1–26. doi:10.1002/joc.859.

Chase, T. N., Wolter,K., Roger A. P., & Ichtiaque R. (2006). Was the 2003 European Summer Heat Wave Unusual in a Global Context? Geophysical Research Letters 33 (23): n/a–n/a. doi:10.1029/2006GL027470.

Eclipse Foundation, Azavea, and contributors. (2016). GeoTrellis, Apache 2.0 License. https://github.com/locationtech/geotrellis.

United Nations, Department of Economic and Social Affairs, Population Division. (2014). World Urbanization Prospects: The 2014 Revision, Highlights (St/Esa/Ser. a/352). United Nations New York, NY, USA.

Hansen, J., Ruedy, R., Sato, M., & ?K. Lo.? (2010). GLOBAL Surface Temperature Change. Reviews of Geophysics 48 (4). doi:10.1029/2010RG000345.

Hassid, S., Santamouris, M., Papanikolaou, N., Linardi, A., Klitsikas N., Georgakis C., & Assimakopoulos, D.N. (2000). The Effect of the Athens Heat Island on Air Conditioning Load. Energy and Buildings 32 (2): 131–41. doi:http://dx.doi.org/10.1016/S0378-7788(99)00045-6.

Hijmans, Robert J. (2016). Raster: Geographic Data Analysis and Modeling. https://CRAN.R-project.org/package=raster.

Kratzer, A. (1937). Das Stadtklima. Die Wissenschaft, Einzeldarstellungen aus der Naturwissenschaft und der Technik, Band 90. ?JSTOR.?

Krige, D. G. (1951). A Statistical Approach to Some Basic Mine Valuation Problems on the Witwatersrand. Journal of the Southern African Institute of Mining and Metallurgy 52 (6). Southern African Institute of Mining; Metallurgy: 119–39.

Martin, P., Baudouin Y., & Gachon, P. (2015). An Alternative Method to Characterize the Surface Urban Heat Island. International Journal of Biometeorology 59 (7): 849–61. doi:10.1007/s00484-014-0902-9.

Menberg, K., Bayer P., Zosseder, K., Rumohr, S., &Blum, P. (2013). Subsurface Urban Heat Islands in German Cities. The Science of the Total Environment 442: 123–33. doi:10.1016/j.scitotenv.2012.10.043.

Moran, P. (1950). Notes on Continuous Stochastic Phenomena. Biometrika, 37(1/2), 17-23. doi:10.2307/2332142

Oke, T.R. (1982). The Energetic Basis of the Urban Heat Island. Quarterly Journal of the Royal Meteorological Society 108 (455). Wiley Online Library: 1–24.

Oliver, M. A., &Webster, R. (1990). Kriging: A Method of Interpolation for Geographical Information Systems. International Journal of Geographical Information Systems 4 (3): 313–32. doi:10.1080/02693799008941549.

Ord, J. K., & Getis, A. (1995). Local Spatial Autocorrelation Statistics: Distributional Issues and an Application. Geographical Analysis 27. doi:10.1111/j.1538-4632.1995.tb00912.x.

Pulugurtha, Srinivas S, Vanjeeswaran K Krishnakumar, and Shashi S Nambisan. (2007). New Methods to Identify and Rank High Pedestrian Crash Zones: An Illustration. Accident Analysis & Prevention 39 (4). Elsevier: 800–811.

Schwarz, N., Lautenbach, S., & Seppelt, R. (2011). Exploring Indicators for Quantifying Surface Urban Heat Islands of European Cities with Modis Land Surface Temperatures. Remote Sensing of Environment 115 (12): 3175–86. doi:10.1016/j.rse.2011.07.003.

Schwarz, N., Schlink, U., Franck, U., & Großmann, K. (2012). Relationship of Land Surface and Air Temperatures and Its Implications for Quantifying Urban Heat Island Indicators—An Application

for the City of Leipzig (Germany). Ecological Indicators 18: 693–704. doi:10.1016/j.ecolind.2012.01.001.

Stewart, I. D., & Oke, T.R. (2012). Local Climate Zones for Urban Temperature Studies. Bulletin of the American Meteorological Society 93 (12): 1879–1900. doi:10.1175/BAMS-D-11-00019.1.

Thakali, L., Kwon, T.J., & Liping Fu. (2015). Identification of crash hotspots using kernel density estimation and kriging methods: a comparison. Journal of Modern Transportation 23 (2). Springer Berlin Heidelberg: 93–106. doi:10.1007/s40534-015-0068-0.

Tomlin, C.D. (1990). Geographic Information Systems and Cartographic Modeling. Prentice Hall Series in Geographic Information Science. Prentice Hall.

Xie, Yihui. (2014). Knitr: A Comprehensive Tool for Reproducible Research in R. Chapman; Hall/CRC. http://www.crcpress.com/product/isbn/9781466561595.

Ye, Xiaofang, Rodney Wolff, Weiwei Yu, Pavla Vaneckova, Xiaochuan Pan, & Shilu Tong. (2012). Ambient Temperature and Morbidity: A Review of Epidemiological Evidence. Environmental Health Perspectives 120 (1): 19–28. doi:10.1289/ehp.1003198.